RE-ENTRY DISPOSAL ANALYSIS FOR LIBRATION POINT ORBIT MISSIONS

Elisa Maria Alessi[(1)], Camilla Colombo[(2)], and Markus Landgraf[(3)]
[(1)]*IFAC–CNR, Via Madonna del Piano 10, 50019 Sesto Fiorentino (FI), Italy, +39 055 5226315, em.alessi@ifac.cnr.it*
[(2)]*Politecnico di Milano, Department of Aerospace Science and Technology, Via La Masa 34, 20156 Milano, Italy, +39 02 23998370, camilla.colombo@polimi.it*
[(3)]*ESA/ESOC, Robert-Bosch-Str. 5, 64293 Darmstadt, Germany, +49 6151 903627, Markus.Landgraf@esa.int*

Abstract:

Nowadays, the mission design comprises the implementation of end-of-life disposal solutions to preserve the space environment. These solutions must be conceived as feasible, sustainable and not demanding from the point of view of the operations. In this work, the Earth's re-entry is presented as a promising disposal strategy to be adopted at the end-of-life of Libration Point Orbit missions, following a recent ESA study. The analysis is performed selecting as test cases Herschel, SOHO and Gaia. We first exploit the natural dynamics corresponding to the Circular Restricted Three–Body Problem and then we develop, within a full dynamical model, a differential correction procedure aimed at computing the precise maneuver which allows reaching the Earth. We pay attention not only on the $\Delta v-$budget, but also to the re-entry angle, the time of flight and the regions on the surface of the Earth affected by the re-entry.

Keywords: *Disposal Strategy, Libration Point Orbits, Re-entry.*

1. Introduction

Since the end of the 70's, the neighborhood of the Sun–Earth libration points L_1 and L_2 has been recognized as a vantage location for Sun's observation and astrophysics purposes, respectively. It is known that nominal L_1/L_2 either periodic or quasi-periodic orbits revolve around the Sun at a distance of about 1.5×10^6 km with respect to the Earth and are designed, in a first approximation, within the Circular Restricted Three–Body Problem (CR3BP) [1]. On one side the multi-body dynamics presents a wider range of bounded solutions compared to the classical Keplerian approach; on the other hand, the unstable character associated with these solutions allows relatively easy and inexpensive transfers.

Recently, the final fate of this kind of missions has drawn the attention of NASA and ESA and some disposal strategies have been implemented to preserve the space environment. Libration Point Orbits (LPO) are not considered 'protected regions', like in the LEO and GEO cases, but it is still a matter of concern their evolution after the achievement of the objectives of the mission. The chaotic dynamics causes the spacecraft to move rapidly off the LPO and, if the trajectory is not driven in a specific way, it may go back to Earth. As we will show here, this eventuality is not necessarily to be avoided, but it should be accurately planned, especially because the spacecraft involved are usually quite large and massive. So far, LPO missions have been either disposed on a graveyard heliocentric orbit, this is the case of ISEE-3, Herschel and Planck, or transferred to

different less exploited CR3BP orbits, like Back-Flip or Distant Prograde Orbits in order to obtain the highest possible scientific return from the payload. In the case of WIND, in particular, this policy permitted a mission extension up to 2067.

In this framework, we are carrying out an ESA study [2, 3] to provide effective decommissioning strategies for some selected LPO missions, taking into account specific constraints and requirements. At the moment, no common end-of-life guidelines exist and one of the objective of the study is to pave the way for future recommendations. As a general rule, the disposal concepts must be conceived as feasible, sustainable and not demanding from the point of view of the operations. Moreover, the solutions must be considered robust in terms of uncertainty on the initial conditions, timing and maneuver application. In case of Earth's re-entry, the collision risk within LEO and GEO regions must be evaluated. The main constraints regard the available propellant on board and the expected area-to-mass ratio at the end-of-life. Having this in mind, there exist three possible disposal options, namely the Earth's re-entry, the lunar impact (both directly and after a weak capture) and the injection into a heliocentric graveyard orbit. In the third case, the spacecraft must be prevented from returning to Earth, as it just happened with ISEE-3, and to ensure that an additional maneuver is mandatory to move the spacecraft on a safe energy regime.

In this work, we will present the analysis on the Earth's re-entry strategy. In a first step, the natural unstable dynamics of the LPO is exploited under the CR3BP assumptions and a differential correction procedure is developed within a full dynamical model, aimed at computing the precise maneuver which allows to reach the Earth. The simplified model is considered because it can be handled with the tools of the dynamical system theory, providing a direct understanding on how to achieve the transfer, together with any possible drawback. As Giuseppe Colombo used to say: 'Before computing an orbit, you have to see it.'. The outcome will be discussed in terms of $\Delta v-$budget, operational effort and re-entry risk.

2. Dynamical Models

As just mentioned, two dynamical models are considered, the CR3BP and a high-fidelity one, which accounts for the gravitational attraction of Sun, Moon and all the planets from Mercury to Pluto, the solar radiation pressure, the atmospheric drag below an altitude of 2000 km and the 10×10 geopotential. In both cases, the numerical integration is done by means of a Runge-Kutta-Fehlberg method of orders 7 and 8.

2.1. Circular Restricted Three–Body Problem

It is known that the CR3BP studies the behavior of a particle with negligible mass which is assumed to move under the gravitational attraction of two primaries of masses m_1 and m_2, which revolve around their common center of mass on circular orbits. In this work, m_1 is the Sun, m_2 the Earth–Moon barycenter. To remove time dependence from the equations of motion, it is convenient to introduce a synodic reference system $\{O,x,y,z\}$, which rotates around the $z-$axis with constant angular velocity equal to the mean motion of the primaries. The origin of the reference frame is set at the barycenter of the system and the $x-$axis on the line joining the primaries, oriented in the direction of the smallest primary. In this way m_1 and m_2 result to be fixed on the $x-$axis.

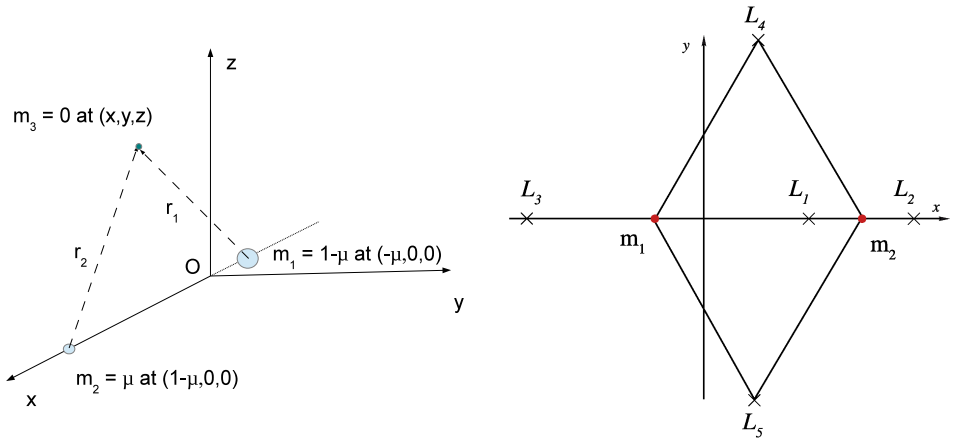

Figure 1. The synodic reference system for the CR3BP and the equilibrium points (right).

The units are chosen to set the gravitational constant, the sum of the masses of the primaries, the distance between them and the modulus of the angular velocity of the rotating frame equal to 1. In the Sun–Earth+Moon system, the unit of distance equals 1 AU = 1.49597870691×10^8 km and the dimensionless mass of the Earth+Moon barycenter is $\mu = \frac{m_2}{m_1+m_2} = 3.0404234\times10^{-6}$. In this way, the most massive body is located at $(-\mu,0,0)$, the second one at $(1-\mu,0,0)$ (see Fig. 1) and the equations of motion read

$$\begin{aligned} \ddot{x}-2\dot{y} &= x-\frac{(1-\mu)}{r_1^3}(x+\mu)-\frac{\mu}{r_2^3}(x-1+\mu), \\ \ddot{y}+2\dot{x} &= y-\frac{(1-\mu)}{r_1^3}y-\frac{\mu}{r_2^3}y, \\ \ddot{z} &= -\frac{(1-\mu)}{r_1^3}z-\frac{\mu}{r_2^3}z, \end{aligned} \tag{1}$$

where $r_1 = [(x+\mu)^2+y^2+z^2]^{\frac{1}{2}}$ and $r_2 = [(x-1+\mu)^2+y^2+z^2]^{\frac{1}{2}}$ are the distances between the particle and the two primaries. This system of equations has a first integral, the Jacobi integral, which is given by

$$(x^2+y^2)+2\frac{1-\mu}{r_1}+2\frac{\mu}{r_2}+(1-\mu)\mu-\left(\dot{x}^2+\dot{y}^2+\dot{z}^2\right)=C_J, \tag{2}$$

where C_J is the so called Jacobi constant.

In the synodic reference system, there exist five equilibrium (or libration) points (see Fig. 1), whose central dynamical behavior defines periodic and quasi-periodic orbits in their neighborhood, namely the libration point orbits [4]. The collinear points L_1, L_2, L_3 are also characterized by one hyperbolic component and thus stable and unstable invariant manifolds arise from the corresponding LPO [5, 6, 7]. Each manifold is characterized by two branches, one going towards the smallest primary, the other on the opposite direction. They look like tubes of asymptotic trajectories tending to, or departing from, the corresponding orbit for positive time. In what follows, the design of the re-entry is established on the unstable invariant manifold of the nominal LPO. The associated

initial conditions are computed, in a first approximation, by moving off from the LPO along the unstable eigendirection (see, for instance, [8]). The variational equations are implemented to this end.

2.2. Full Ephemeris Model

The equations of motion of the full dynamical model are written in the geocentric equatorial reference system $\{O,\xi,\eta,\zeta\}$ and physical units of distance, time and mass (AU, day and kg) are used. The behavior of the spacecraft depends on different contributions listed in what follows.

The gravitational acceleration (subscript g) exerted on the spacecraft by Sun, Moon and the planet is modeled as

$$\begin{aligned}
\ddot{\xi}_g &= -\sum_{p=1}^{11} Gm_p \frac{(x_E - x_p + \xi)}{r_{Ep}^3} - \ddot{x}_E, \\
\ddot{\eta}_g &= -\sum_{p=1}^{11} Gm_p \frac{(y_E - y_p + \eta)}{r_{Ep}^3} - \ddot{y}_E, \\
\ddot{\zeta}_g &= -\sum_{p=1}^{11} Gm_p \frac{(z_E - z_p + \zeta)}{r_{Ep}^3} - \ddot{z}_E,
\end{aligned} \tag{3}$$

where

- $(x_p, y_p, z_p, \dot{x}_p, \dot{y}_p, \dot{z}_p)$ is the state vector in the equatorial reference system centered at the Solar System barycenter of the body P of mass m_p and it is evaluated, at a given instant of time, from the JPL ephemeris DE405 [9];
- $(x_E, y_E, z_E, \dot{x}_E, \dot{y}_E, \dot{z}_E)$ is the Earth's state vector in the equatorial reference system centered at the Solar System barycenter and it is also given by the JPL ephemeris DE405 at each instant of time;
- $r_{Ep} = \sqrt{(x_E - x_p + \xi)^2 + (y_E - y_p + \eta)^2 + (z_E - z_p + \zeta)^2}$.

The effect due to the solar radiation pressure (subscript *SRP*) follows the so-called cannonball model and can be seen as the effect due to a residual mass of the Sun, namely,

$$\begin{aligned}
\ddot{\xi}_{SRP} &= -C_R \bar{P} a_\odot^2 \frac{A}{m} \frac{(x_E - x_S + \xi)}{r_{ES}^3} \\
\ddot{\eta}_{SRP} &= -C_R \bar{P} a_\odot^2 \frac{A}{m} \frac{(y_E - y_S + \eta)}{r_{ES}^3}, \\
\ddot{\zeta}_{SRP} &= -C_R \bar{P} a_\odot^2 \frac{A}{m} \frac{(z_E - z_S + \zeta)}{r_{ES}^3},
\end{aligned} \tag{4}$$

where C_R is the reflectivity coefficient, $\bar{P} = 4.51 \times 10^{-6}$ N/m^2 is the mean solar radiation pressure at 1 AU, $a_\odot = 1$ AU is the mean distance between the Sun and the Earth, A/m is the ratio-to-mass ratio and the subscript S denotes the Sun.

Whenever the spacecraft orbits below an altitude of 2000 km, the acceleration due to the atmo-

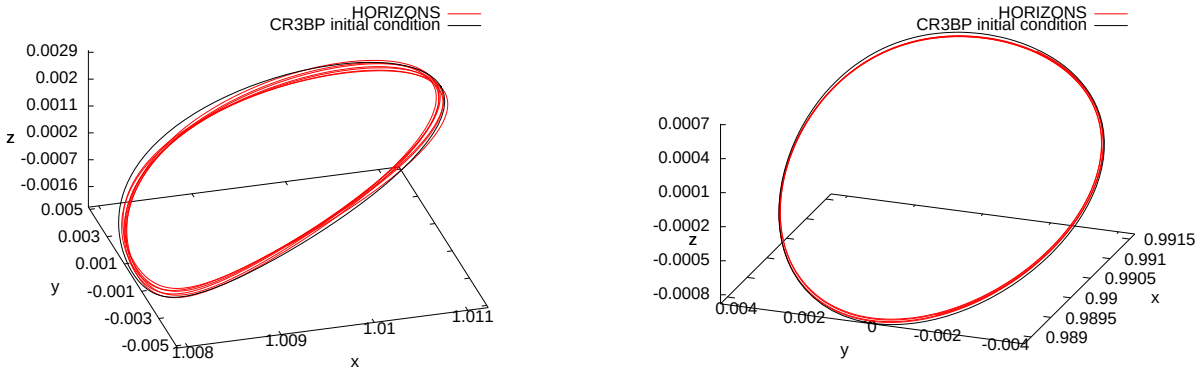

Figure 2. **The orbit provided by the JPL HORIZONS system together with the one used in our simulations. Non dimensional units, synodic reference system centered at the Sun-Earth+Moon barycenter. Left: Herschel. Right: SOHO.**

spheric drag (subscript ATM) is taken into account, namely,

$$\mathbf{a}_{ATM} = -\frac{1}{2} C_D \rho \frac{A}{m} v_a^2 \hat{\mathbf{v}}_\mathbf{a} \tag{5}$$

where $C_D = 2.2$ is the drag coefficient, $\mathbf{v}_a$ is the relative satellite-atmosphere velocity, assuming that the atmosphere rotates together with the Earth with angular velocity of modulus $w_\oplus = 4.178 \times 10^{-3}$ deg/s, and ρ is the atmospheric density, which is modeled by the static isotherm exponential model [10].

Concerning the geopotential, we adopt the formulation in Cartesian body-fixed coordinates described in [11]. The Earth's rotation to obtain the acceleration in the inertial reference system is given by the Software Routines from the IAU SOFA Collection [12] and the coefficients used correspond to the EGM96 model.

In this model, the variational equations are implemented in view of the differential correction procedure (see Sec. 4.2.). They actually correspond to the central gravitational acceleration and to the solar radiation pressure, but not to the other two effects considered. As we will see, the maneuver is applied at an altitude where the latter can be considered as negligible.

3. Test Cases

The LPO missions selected for this work are Herschel, SOHO and Gaia. The nominal orbit of Herschel is a L_2 quasi-halo orbit with maximum out-of-plane amplitude of about 450000 km. It is proposed as a reference mission, because it just ended and thus it gives the opportunity to compare our disposal strategy with the solution selected by ESA. The nominal orbit of SOHO is a L_1 halo orbit with maximum out-of-plane amplitude of about 120000 km. It is selected because it is currently orbiting around L_1 and its expected end is in 2016. Finally, Gaia has just been launched on a L_2 Lissajous orbit with a small out-of-plane amplitude, about 90000 km. It can pave the way for new mission concepts by using a pre-planned disposal strategy.

Table 1. **Initial conditions chosen for simulating the behavior of Herschel and SOHO in the CR3BP framework. Non dimensional units, synodic reference system centered at the Sun–Earth+Moon barycenter. T is period of the orbit, C_J the Jacobi constant.**

Mission	LPO	T	x	y	z	$\dot{x}$	$\dot{y}$	$\dot{z}$	C_J
Herschel	L_2 Halo North	3.0947685	1.0111842	0	0.0028010	0	-0.0100059	0	3.0007831
SOHO	L_1 Halo South	3.0595858	0.9888381	0	-0.0008802	0	0.0089580	0	3.0008294

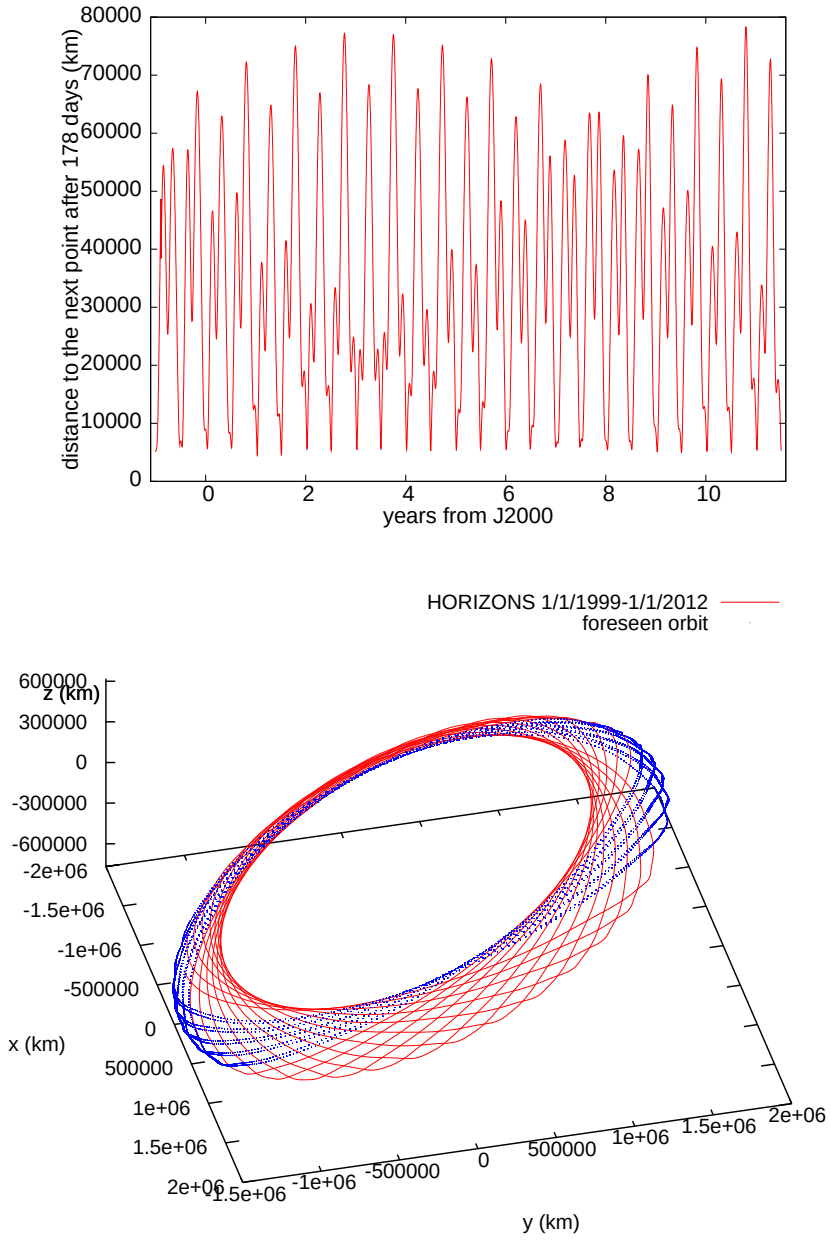

Figure 3. **Top: difference in position between points belonging to the actual orbit of SOHO distanced by 178 days, from January 1, 1999 at 00:00 to July 8, 2011 at 00:00. Bottom: the orbit of SOHO, in the geocentric equatorial reference system, as foreseen in the future, assumed to be periodic in the synodic CR3BP reference frame with period equal 178 days.**

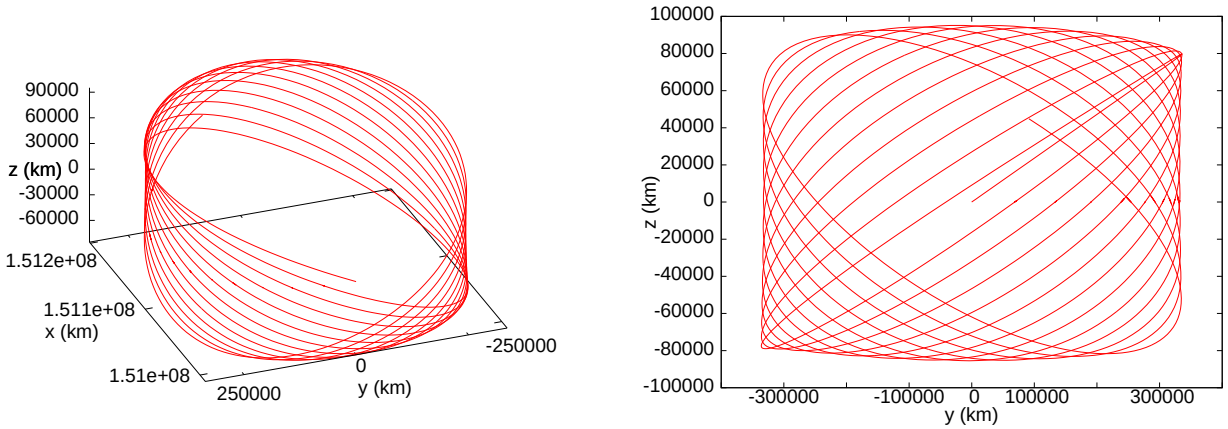

Figure 4. **Lissajous orbit considered to simulate the evolution of Gaia. Left: 3D representation. Right:** $y-z$ **projection. Synodic reference system centered at the Sun–Earth+Moon barycenter.**

The period, initial conditions and energy level of the LPO corresponding to Herschel and SOHO, used in the CR3BP framework, are reported in Tab. 1. They were computed by comparison with the actual orbit of the given spacecraft as provided by the JPL HORIZONS system (see Fig. 2). In the full model, the initial position and velocity for Herschel considered are the ones provided by JPL HORIZONS in the time span going from August 31, 2012 at 18:00 to April 29, 2013 at 18:00 with one-day step. For SOHO, the latest available data from JPL HORIZONS were used, which cover the time interval going from January 1, 2011 at 00:00 to January 1, 2012 at 00:00. Also in this case, the data were taken with one-day time step. These dates do not reflect the expected end-of-life for SOHO, but they were used to simulate the future orbit of the mission until November 15, 2016 at 00:48 and then compute the final re-entry. To be precise, its orbit is assumed to be periodic in the synodic CR3BP reference frame with period equal 178 days. This approximation turns out to be a good initial guess for the future behaviour of the spacecraft. As a verification, Fig. 3 (top) shows the difference in position between points belonging to the actual orbit of SOHO distanced by 178 days, from January 1, 1999 at 00:00 to July 8, 2011 at 00:00. Fig. 3 (bottom) represents, in the geocentric equatorial reference system, the orbit of SOHO as foreseen in the future with the just mentioned assumption.

The nominal orbit assumed for Gaia is the one shown in Fig. 4 in the synodic reference frame; this is a Lissajous quasi-periodic orbit propagated for about 6 years. This value accounts for the 5.5 years of nominal duration of the mission, plus 6 months set as additional time to start the re-entry phase. The initial conditions considered are the ones provided by the CR3BP approximation, using a Fourier series parametrization as explained in [13]. For the full model simulations, the orbit is transformed into the equatorial geocentric reference frame. Two initial epochs for the first point on the Lissajous orbit were assumed, namely December 24, 2013 at 00:00 and January 23, 2014 at 00:00. As a matter of fact, initially the launch was scheduled on November 20, 2013, but on October 22, 2013 it was announced its postponement due to technical reasons. The time of flight to the libration point orbit was expected to be of about 1 month. The re-entry can take place towards the end of the mission; in the first case from the point on the orbit associated with March 28, 2018 at 00:00, in the second case about 1 month later.

Table 2. Estimated constraints at the end-of-life.

Mission	Δv (m/s)	A/m (m^2/kg)	C_R
Herschel	180	0.0048	1.5
SOHO	143	0.0196	1.9
Gaia	10	0.0585	1.21

With respect to the constraints on $\Delta v-$ budget, A/m and reflectivity coefficient C_R at the end-of-life, their values are reported in Tab. 2. These data were derived after a thorough analysis on the initial mass, propellant consumption, type of structures and relative reflectivity coefficients. We notice in particular that Gaia will have almost no propellant left at the end-of-life.

4. Earth's Re-entry

Due to the massive size of all the considered missions (between 2 and 4 tons), the final phase of a re-entry trajectory should be at least semi-controlled with known orbital parameters at the atmosphere's interface. In particular the re-entry velocity and re-entry angle should be targeted so that the mass surviving the re-entry and the footprints of the fragments are both minimized. In this work, the re-entry angle γ characterizing the final re-entry phase is computed as

$$\tan\gamma = \frac{e\sin\nu}{1+e\cos\nu}, \tag{6}$$

where e and ν are respectively the eccentricity and the true anomaly of the osculating orbit with respect to the Earth at 100 km.

A detailed literature review exists for re-entry from LEO, however very little work is available on re-entry of spacecraft from LPO. In particular, from an analysis of the available literature performed in [14], for LEO spacecraft of around 1000 kg mass, an optimal re-entry angle is found to be -1°. Such value represents a good compromise which minimizes the ground casualty risk, which should be below the IADC accepted level of 10^{-4}. While, as it will be shown, the re-entry velocity is quite constant for LPO re-entry, when selecting the re-entry angle, the two safety requirements are in contradiction because the mass surviving the re-entry is minimized if the magnitude of the re-entry angle is small (i.e., shallow) as the spacecraft experiences a stronger interaction with the atmosphere, but, on the other side, a small re-entry angle increases the footprint of the re-entry fragments. This was shown in [14] in the case of Highly Elliptical Orbits (HEO), that present velocity values comparable with the one of LPO. For HEO, the melting temperature for the spacecraft are reached at lower altitude for steeper re-entry angle. Since fragmentations at very low altitude are expected to be dangerous, a less steep angle should be preferred.

4.1. CR3BP Design

Let us consider the unstable invariant manifolds associated with the nominal LPO of the selected missions, see Tab. 1. As it can be inferred from Fig. 5, they provide a direct transfer to the Earth in the case of Herschel and SOHO. For Gaia, instead, the minimum geocentric distance attained by these trajectories is about 37000 km. This is particularity of the small Lissajous orbits and applies to other missions like Planck. Thus, in principle, only for Gaia an impulsive procedure is required.

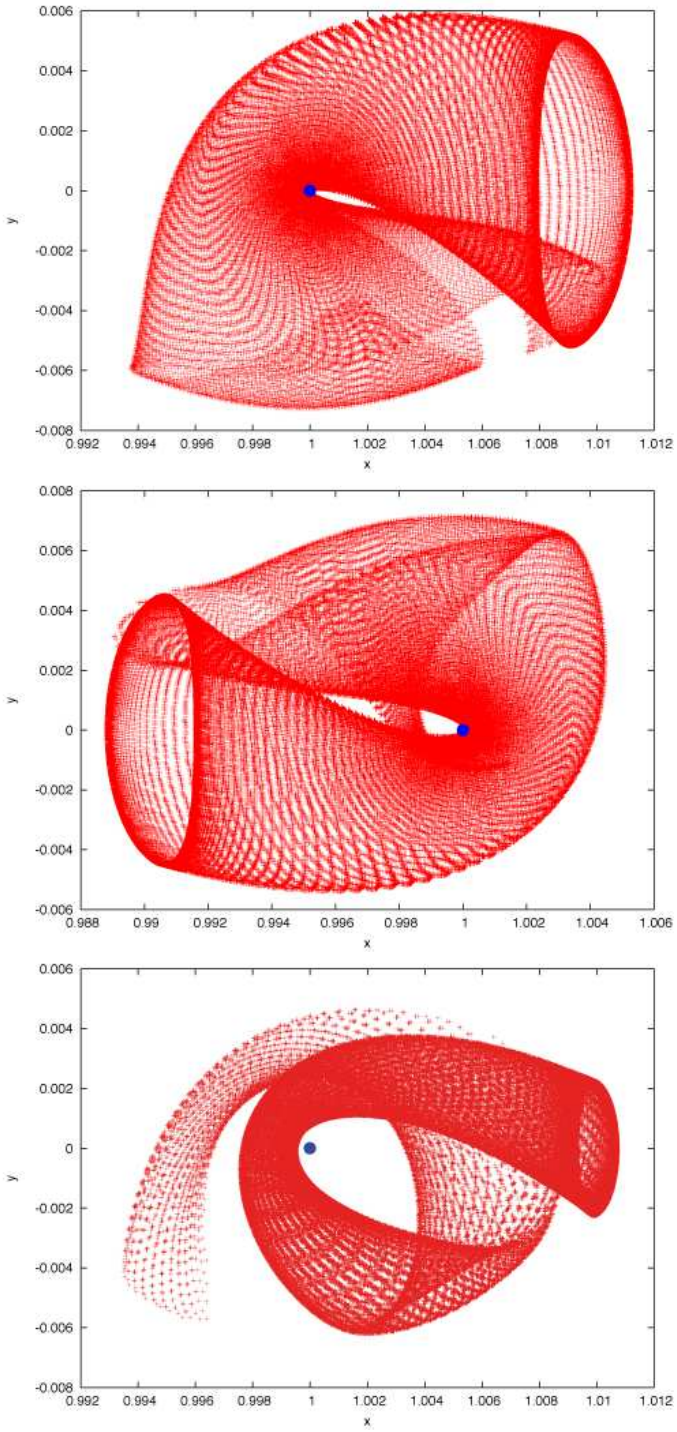

Figure 5. **From top to bottom, unstable invariant manifold of the nominal orbit of Herschel, SOHO and Gaia leading to Earth (blue). Non dimensional units, synodic reference system centered at the Sun–Earth+Moon barycenter.**

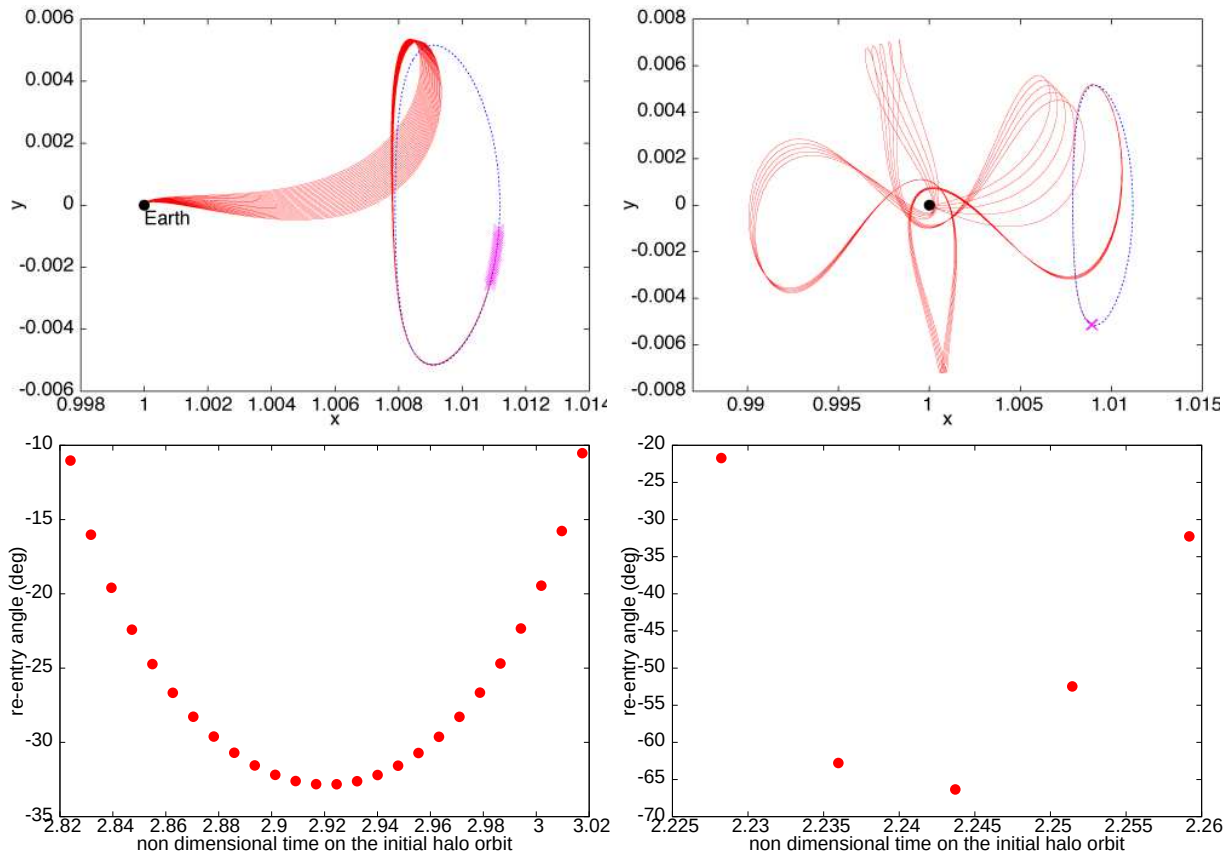

Figure 6. **According to the phase of departure and the type of trajectory, the angle of re-entry changes, if the design is done within the CR3BP model. Top: two kinds of re-entry trajectories for Herschel in the synodic Sun–Earth+Moon reference system (in purple the initial condition). Bottom: The corresponding behavior of the angle of re-entry as a function of the initial phase.**

4.1.1. Herschel and SOHO

The no-cost transfers that can be designed for Herschel and SOHO by means of the unstable invariant manifold can be either direct or not, in the sense that the spacecraft may achieve re-entry after some revolutions at the Earth on highly elliptical orbits (see Figs. 6 and 7). Moreover, the values of re-entry angle γ computed at 100 km of altitude range from $-70°$ to $0°$ and for a given transfer this is function of the initial phase of departure from the LPO and the shape of the trajectory, see Figs. 6 and 7. For Herschel, the first opportunity to re-entry arises after 186 days and later on after 465 days since departure. For SOHO, the re-entry can take place either about 310 days of journey from the nominal LPO or after traveling for 150 days further. The re-entry velocity is about 11.06 km/s at 100 km of altitude, value that can be associated with the Earth's escape velocity. Indeed, the trajectories on the unstable manifold belong to low-energy regimes and, because of that, the re-entry path follows a parabolic orbit.

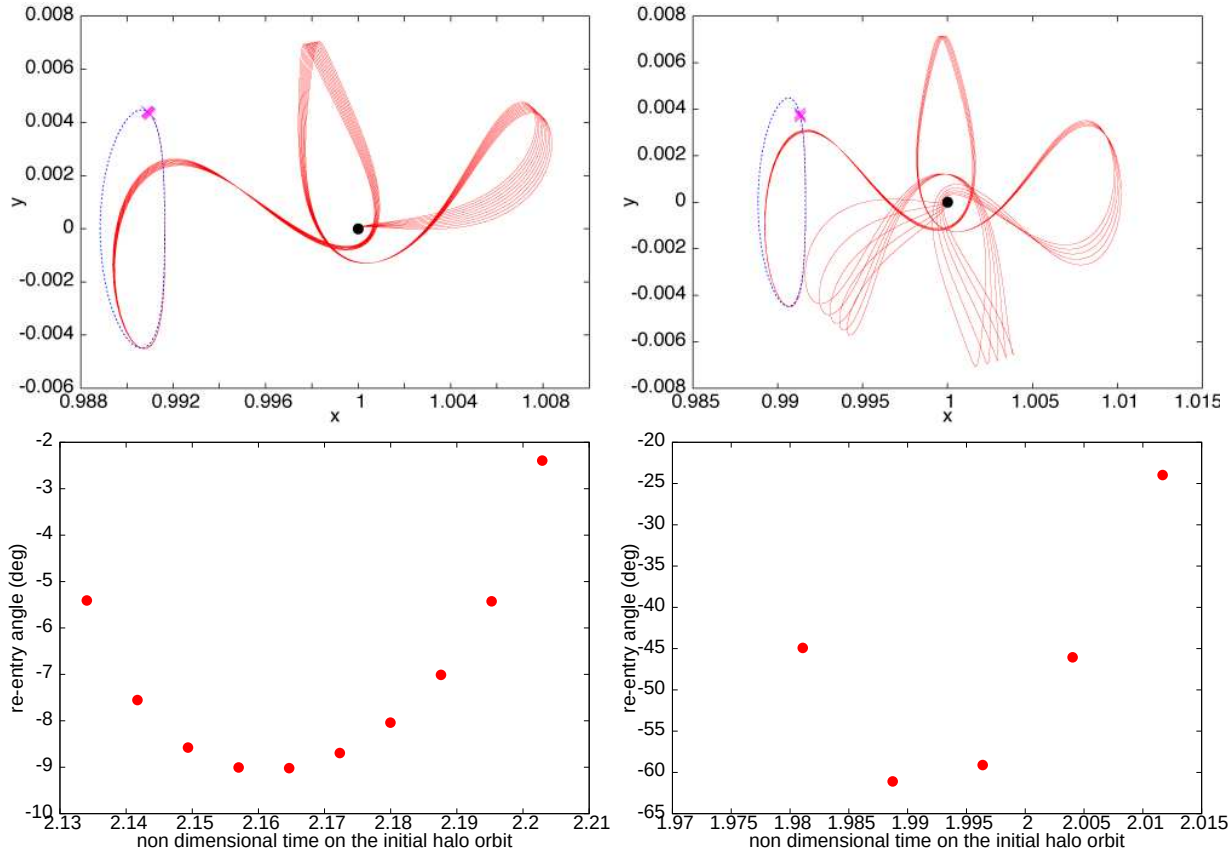

Figure 7. **According to the phase of departure and the type of trajectory, the angle of re-entry changes, if the design is done within the CR3BP model. Top: two kinds of re-entry trajectories for SOHO in the synodic Sun–Earth+Moon reference system (in purple the initial condition). Bottom: The corresponding behavior of the angle of re-entry as a function of the initial phase.**

4.1.2. Gaia

In the case of Gaia, a differential correction method was developed to figure out the $\Delta v-$budget required as a function of its time of application. It can be sketched as follows (see Fig. 8).

- Each initial condition corresponding to the proper branch of the unstable invariant manifold of the Lissajous orbit is propagated for one year through the CR3BP equations of motion.
- A given trajectory generated in this way is discretized with one-day step.
- In correspondence of each of these nodes a tangential maneuver in the sidereal reference system is applied in order to get to the Earth. The initial guess for this maneuver is given by a Hohmann-like transfer, namely:

$$\Delta v = \sqrt{2\frac{Gm_E}{r_0} - E_t} - \sqrt{2\frac{Gm_E}{r_0} - E_0}, \tag{7}$$

where r_0 is the distance between the center of the Earth and the point on the manifold where the maneuver is applied, $E_t = -Gm_E/(r_0 + r_E)$ being $r_E = 6378.137$ km the equatorial radius of the Earth, $E_0 = -Gm_E/2a$ being a the semi-major axis of the osculating ellipse of

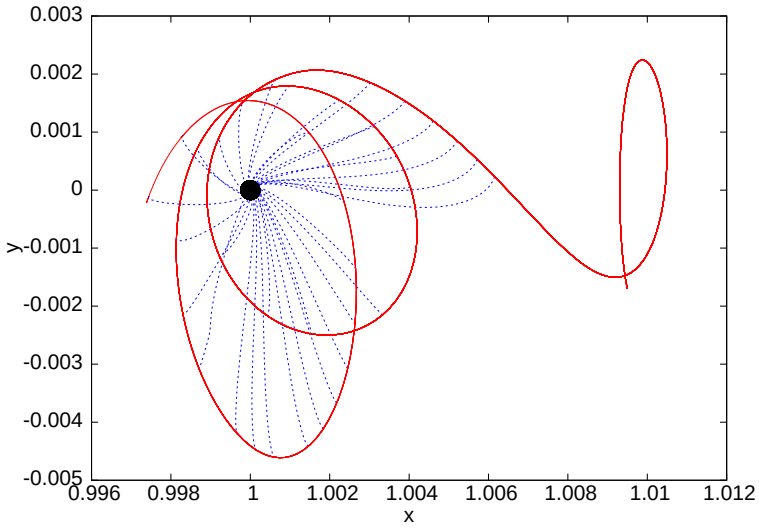

Figure 8. **Schematic example of how the re-entry trajectories are computed for Gaia: a re-entry maneuver at different positions of a given manifold leg is computed by means of the differential correction method. Synodic Sun–Earth+Moon reference system, non dimensional units.**

the point on the manifold.

- After the Δv burn, we look for the minimum of the relative distance between the spacecraft and the Earth. If this does not occur at r_E, then the maneuver is refined by means of the Newton's method.

Concerning the Newton's method, we recall that the radius vector $\mathbf{r}^{sid} \equiv (x^{sid}, y^{sid}, z^{sid})$ of the s/c with respect to the secondary in the sidereal reference system at time t can be derived as

$$\begin{pmatrix} x^{sid} \\ y^{sid} \\ z^{sid} \end{pmatrix} = \mathscr{R} \begin{pmatrix} x+\mu-1 \\ y \\ z \end{pmatrix}, \qquad \text{with} \quad \mathscr{R} = \begin{pmatrix} \cos(t) & -\sin(t) & 0 \\ \sin(t) & \cos(t) & 0 \\ 0 & 0 & 1 \end{pmatrix}, \tag{8}$$

and the velocity vector by deriving (8). If the time derivative of the relative s/c-Earth distance is

$$g = \dot{r_2} = \frac{(x-1+\mu)\dot{x} + y\dot{y} + z\dot{z}}{r_2}, \tag{9}$$

and the section given by the Earth's sphere, that is, the constraint to match, is

$$G = r_2^2 - r_E^2, \tag{10}$$

then the equation to apply reads

$$\nabla G \cdot \mathbf{\Delta X}_0^{sid} \equiv \left[\frac{\partial G}{\partial \mathbf{X}} \cdot (\Phi + \mathbf{F} \cdot \mathbf{Dt}) \frac{\partial \mathbf{X}_0}{\partial \mathbf{X}_0^{sid}} \right] \cdot \mathbf{\Delta X}_0^{sid} = -G, \tag{11}$$

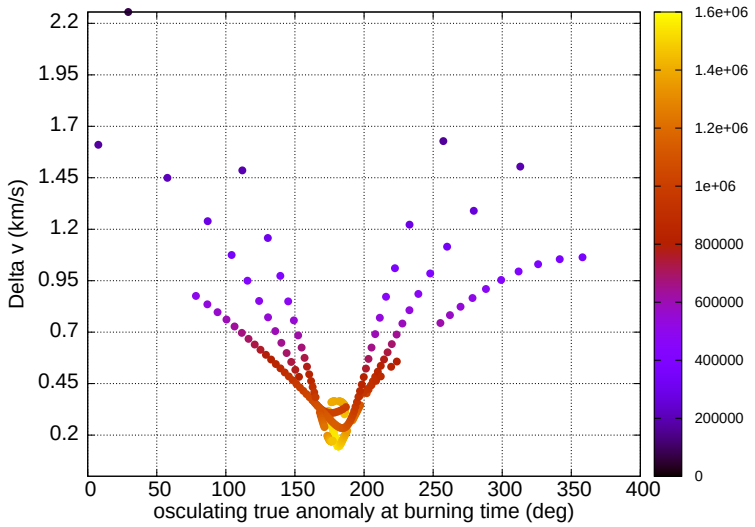

Figure 9. Δv**-budget required to arrive to the Earth for Gaia as a function of the point on the manifold where the maneuver is applied. The color bar reports the Earth-s/c distance (km) at the burning time.**

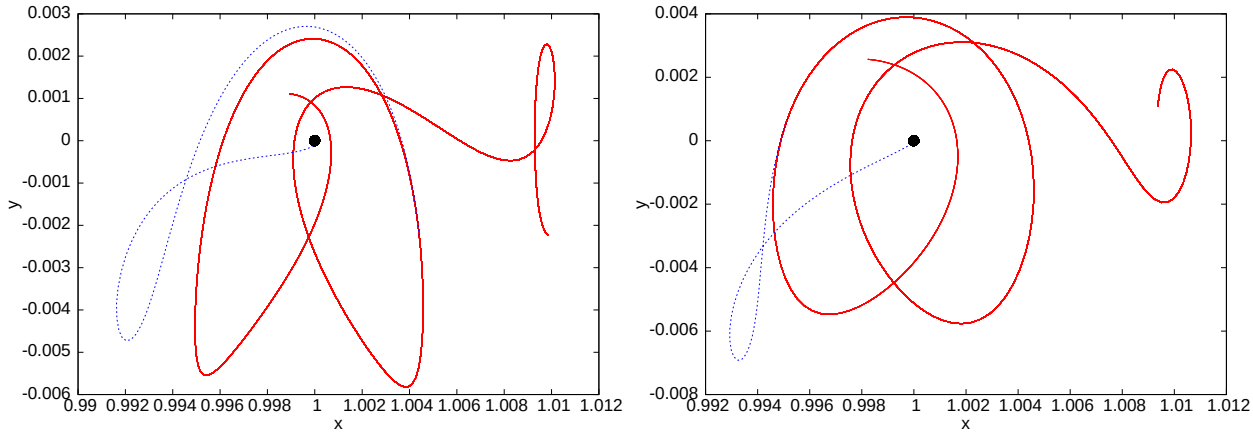

Figure 10. **Examples of low-cost re-entry solutions computed for Gaia. Synodic Sun–Earth+Moon reference system, non dimensional units.**

where $\mathbf{X} \equiv (x, y, z, \dot{x}, \dot{y}, \dot{z})$, $\mathbf{\Delta X}_0^{sid}$ is the correction we apply to the initial conditions in the sidereal reference frame, Φ is the CR3BP variational matrix, $\mathbf{F}$ is the CR3BP vector field, $\mathbf{Dt} = -\frac{\nabla g \cdot \Phi}{\nabla g \cdot \mathbf{F}}$, and

$$\frac{\partial \mathbf{X}_0}{\partial \mathbf{X}_0^{sid}} = \begin{pmatrix} 1 & 0 & 0 & 0 & 0 & 0 \\ 0 & 1 & 0 & 0 & 0 & 0 \\ 0 & 0 & 1 & 0 & 0 & 0 \\ 0 & 1 & 0 & 1 & 0 & 0 \\ -1 & 0 & 0 & 0 & 1 & 0 \\ 0 & 0 & 0 & 0 & 0 & 1 \end{pmatrix}.$$

We notice that, since both the position where the maneuver is applied and the direction of the maneuver are fixed, what Eq. (11) changes is just the value of Δv.

This procedure is able to compute Earth's re-entry trajectories both direct or not, as in the case of Herschel or SOHO. In general, the closer the maneuver is applied at an osculating apogee (and thus the longer the time of flight) the cheaper the transfer, as shown in Fig. 9, but the Δv requirement tends to stay above 150 m/s. However, the approach revealed the existence of low-cost solutions such that $\Delta v < 10$ m/s as the ones shown in Fig. 10. In these situations, the s/c injects into the unstable invariant manifold of different LPO and the whole trajectories were interpreted as either heteroclinic or homoclinic orbits whose time of flight ranges between 100 and 150 days.

4.2. Full Model Design

When considering the full dynamical model, the presence of other forces apart from the gravitational attractions of Sun and Earth+Moon causes the spacecraft to move naturally off the LPO onto the unstable invariant manifold. As this manifold is actually composed by two branches, one leading toward the Earth, the other inward/outward (L_1/L_2) the Solar System, for Herschel and SOHO it may be required to design a maneuver to drive the trajectory along the proper direction. For Gaia, instead, the impulsive burn aims at changing the semi-major axis of a given trajectory on the manifold to ensure the re-entry. This is why we distinguish between the two cases.

4.2.1. Herschel and SOHO

Let us consider the orbit of Herschel and SOHO provided by the JPL ephemeris, as described in Sec. 3.. The differential correction procedure implemented looks for the change in the initial velocity such that the spacecraft joins the Earth-ward branch of the unstable invariant manifold. The methodology is sketched in Fig. 11. A given initial condition is transformed into the non dimensional synodic Sun–Earth+Moon reference system and is propagated through the equations of motion corresponding to the CR3BP for a given time interval, which is chosen between 1 and 30 days. At this point, the spacecraft is expected to inject into the unstable invariant manifold which leads to re-entry. To this end the variational equations of the CR3BP are propagated together with the equations of motion: a Newton's method is applied to correct properly the initial velocity of the LPO in the CR3BP frame. In turn, this results in changing the initial velocity of the LPO in the real ephemerides model. The differential procedure targets the initial condition on the unstable manifold (corresponding to the LPO in Tab. 1) which minimizes such maneuver. In particular, changing the time of flight to get to the manifold modifies both the required maneuver and the point reached on the manifold. In principle, another maneuver would be required to match the manifold also in velocity, but in practice this is not needed. Indeed, the CR3BP allows understanding how to move towards the Earth and, in a second stage, the new initial condition obtained through the differential correction is propagated in the high-fidelity dynamical model.

Whenever an orbit gets to an altitude lower than 100 km in less than a year, the re-entry angle γ is evaluated as explained before. In this way, several re-entry solutions are obtained for the time interval covered by the missions. Among them we selected the ones associated with an initial maneuver smaller than 150 m/s as suggested by Tab. 2 and a re-entry angle in between 0 and -20 degrees. Higher (in absolute magnitude) re-entry angles are possible, but in those cases it is expected that the spacecraft would fragment at a lower altitude, with a consequent higher ground casualty risk [14]. We notice that when the re-entry is designed in the full model, the

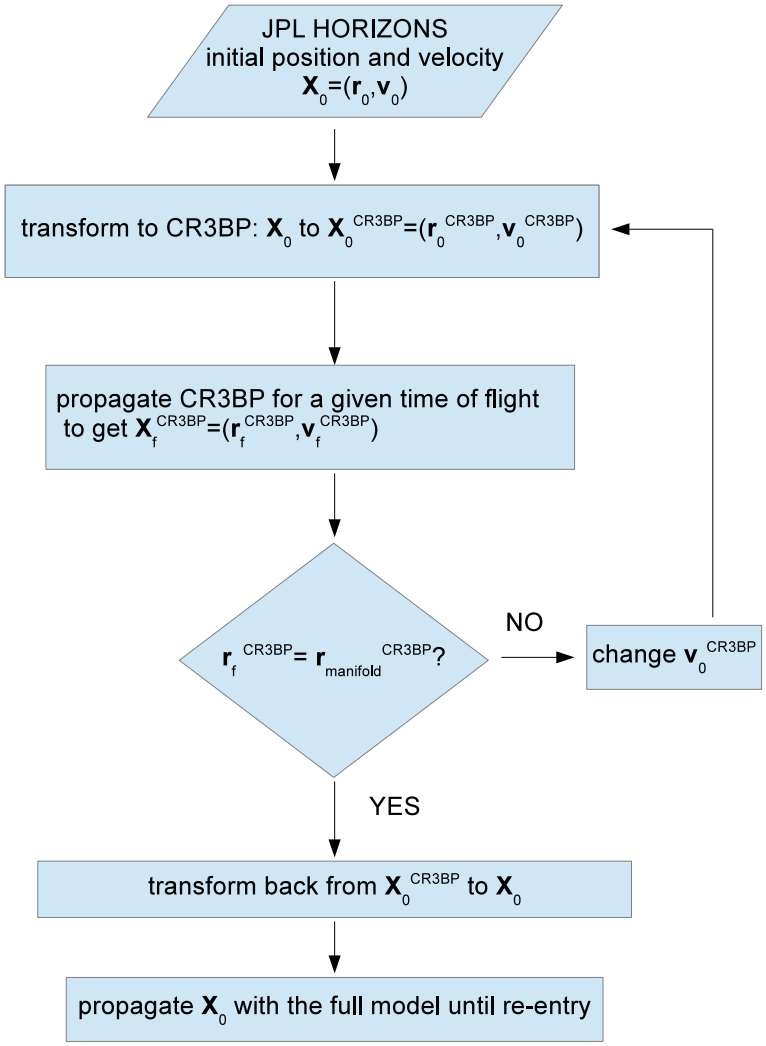

Figure 11. Scheme of the differential procedure implemented for Herschel and SOHO.

correspondence mentioned before between the initial departure phase and the re-entry angle is broken. It looks like that two factors are responsible for that: the initial maneuver and the solar radiation pressure, which indeed are able to modify significantly the trajectories.

The solutions which could be selected for Herschel re-entry are shown in Fig. 12 (left). We notice that none of them take place in 2013 (the year of the actual disposal maneuver for Herschel) because a lower limit of the re-entry angle was fixed to -20 degrees, following the considerations drawn before. Figure 13 (left) represents the ground-track of the six entry conditions (at 100 km) for the solutions represented in Fig. 12 (left). The points are colored based on the re-entry angle (see Fig. 14 left). All the solutions target equatorial latitudes, and some solutions present a re-entry points over an oceanic area. This allows mitigating the ground causality risk. However, in a future study the last phase of the re-entry, for altitude below 100 km, should be analyzed. We also notice that five solutions correspond to direct re-entry (see Fig. 15 left), while one trajectory transfers to

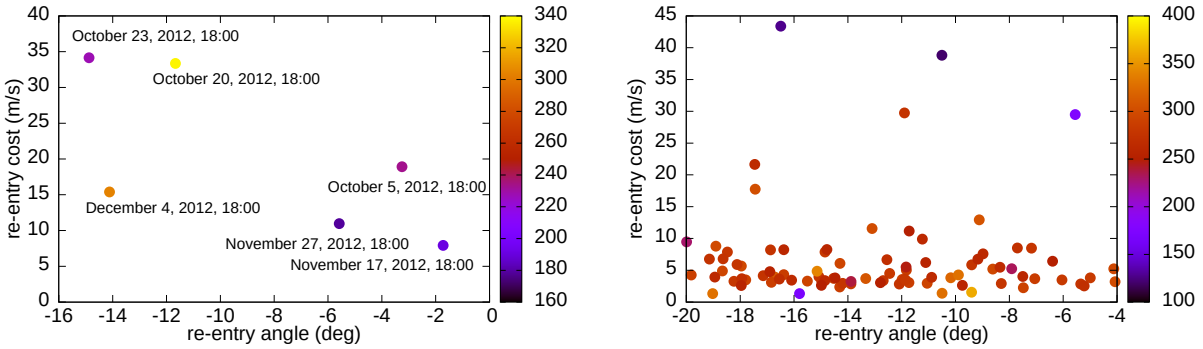

Figure 12. **Final solutions for Herschel and SOHO. The color bar refers to the time of flight (days).**

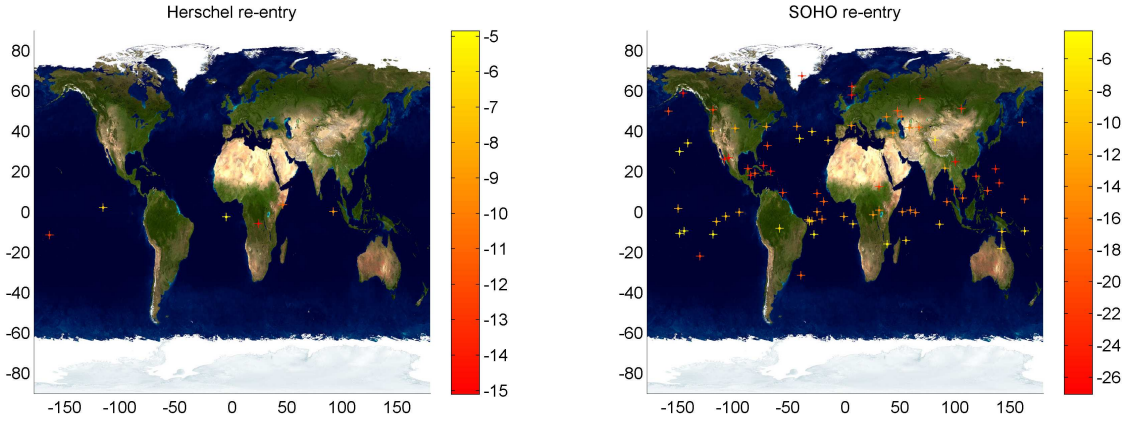

Figure 13. **Ground-track of the entry conditions (at 100 km) for the solutions represented in Fig. 12 for Herschel (left) and SOHO (right). The color bar reports the corresponding angle of re-entry (deg).**

a highly elliptical orbit before re-entering (see Fig. 15 right).

The re-entry disposal trajectories starting from initial conditions generated in the time span between 2014 to the end of 2016 for SOHO are shown in Fig. 12 (right). The higher number of solutions displayed in this case is due to the larger time interval when the re-entry can occur. Also in this case the ground-track of the entry conditions (at 100 km) can be shown, colored based on the re-entry angle (see Figs. 13 and 14 right). In the case of SOHO, not all the solutions target equatorial latitudes or oceanic areas and therefore a further selection of the solutions should be made, based on the ground causality risk. Examples of direct re-entry and transfers to a highly-elliptical orbit before re-entering are shown in Fig. 16 for SOHO.

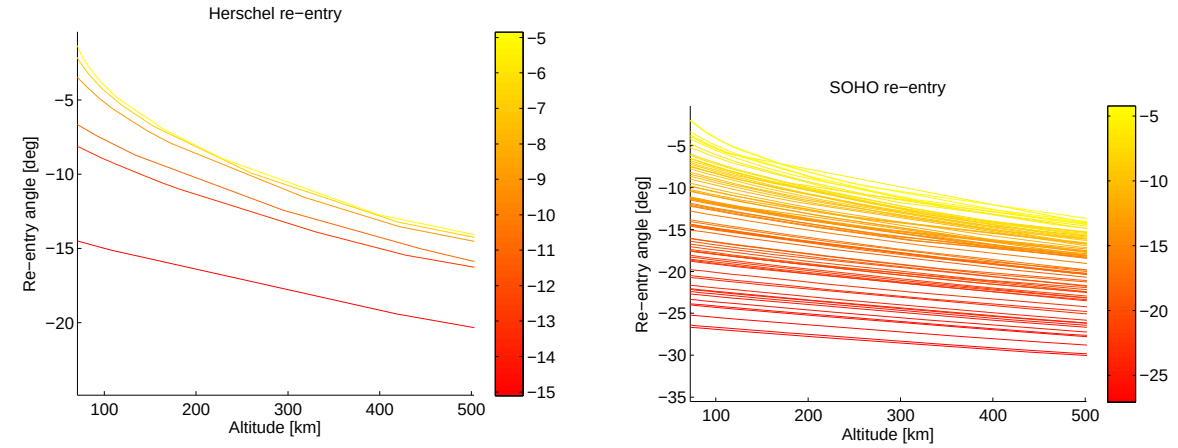

Figure 14. **Behavior of the re-entry angle as a function of the altitude for the solutions proposed for Herschel (left) and SOHO (right). The color bar reports the final angle of re-entry (deg).**

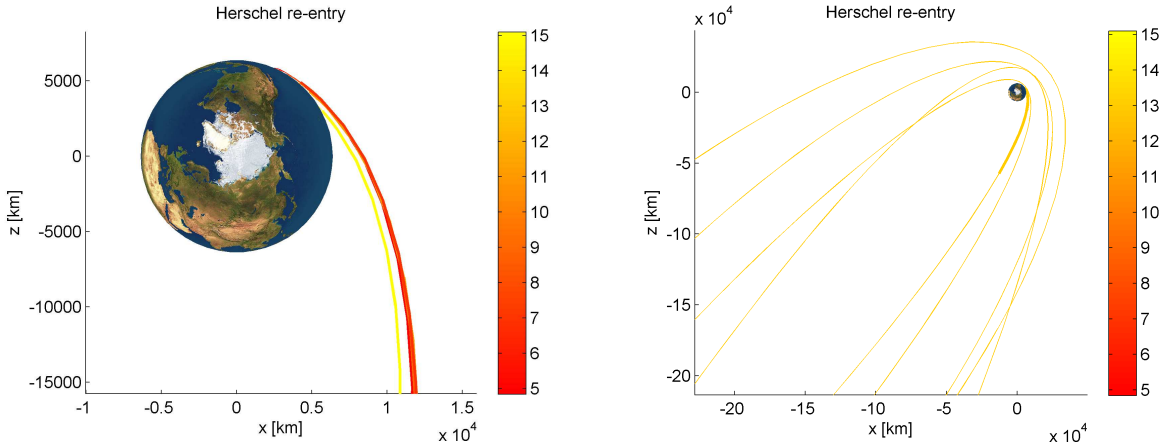

Figure 15. **Direct re-entry solutions (left) and re-entry through transferring on a highly elliptical orbit (right) for Herschel. The color bar reports the angle of re-entry (deg).**

4.2.2. Gaia

As seen before, Gaia cannot re-enter to the Earth naturally. Thus, the differential correction method applied here does not aim at inserting into the unstable manifold but at computing the maneuver which allows the re-entry. This is why the CR3BP dynamical model is not exploited (apart for generating the initial conditions), but the equations of motion of the high-fidelity model and the corresponding variational equations were used straight away. In principle, the same strategy could be implemented also for Herschel and SOHO to look for zero-cost transfers. However, as the solutions provided in those cases are really not expensive (especially in the case SOHO for which most of the transfers require less than 10 m/s) we consider the two procedures equivalent.

The differential correction method developed is analogous to the one described in Sec. 4.1.2., the only difference is that now each initial condition on the Lissajous orbit is transformed into the geocentric equatorial reference system at the beginning of the procedure and in Eq. (11) we do not

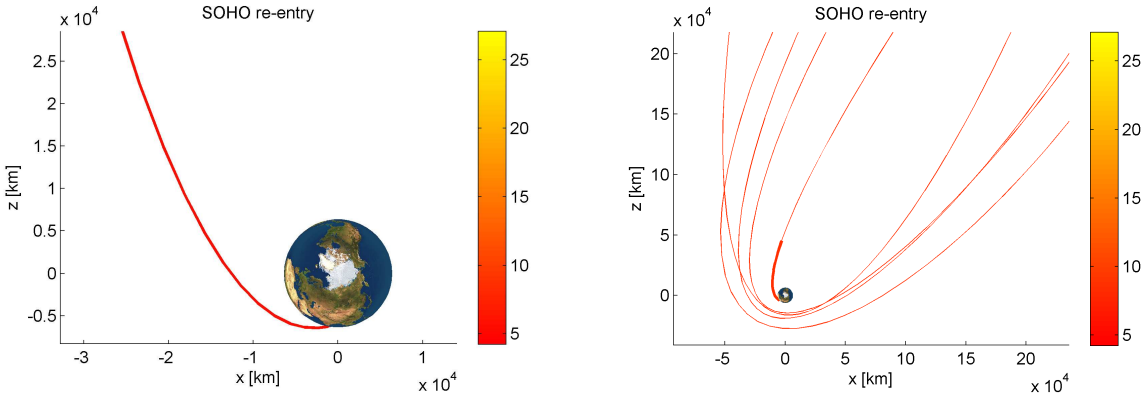

Figure 16. **Example of direct re-entry solutions (left) and re-entry through transferring on a highly elliptical orbit (right) for SOHO. The color bar reports the angle of re-entry (deg).**

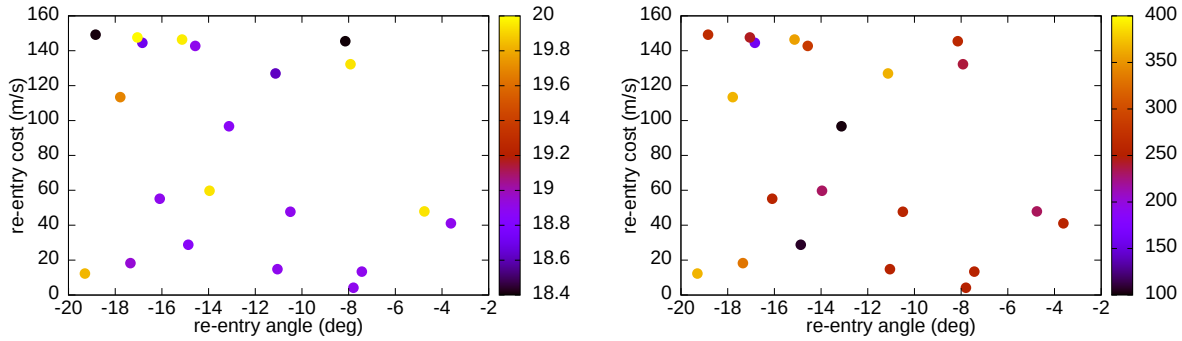

Figure 17. **Optimal solutions found for Gaia re-entry in terms of re-entry cost (m/s) and re-entry angle (deg), being the initial epoch on the LPO on December 24, 2013 at 00:00. The color bar on the left reports the initial epoch of the re-entry trajectory (left) and the total time of transfer in days (right).**

need to distinguish between sidereal and synodical coordinates.

Figures 17 and 18 show the feasible solutions in terms of re-entry angle, Δv cost, time of flight and initial epoch. We accept the solutions corresponding to apogee burning maneuver and the ones deriving from either heteroclinic or homoclinic connections. In Fig. 19 we show the regions on the Earth's surface involved by the re-entry for all the low-cost trajectories no matter on the re-entry angle, assuming as initial epoch on the LPO January 23, 2014 at 00:00.

5. Conclusions

Herschel's science mission ended on April 29, 2013 due to the helium coolant's exhaustion. The spacecraft was kept active until June 2013 to perform technology and operations tests and thus take

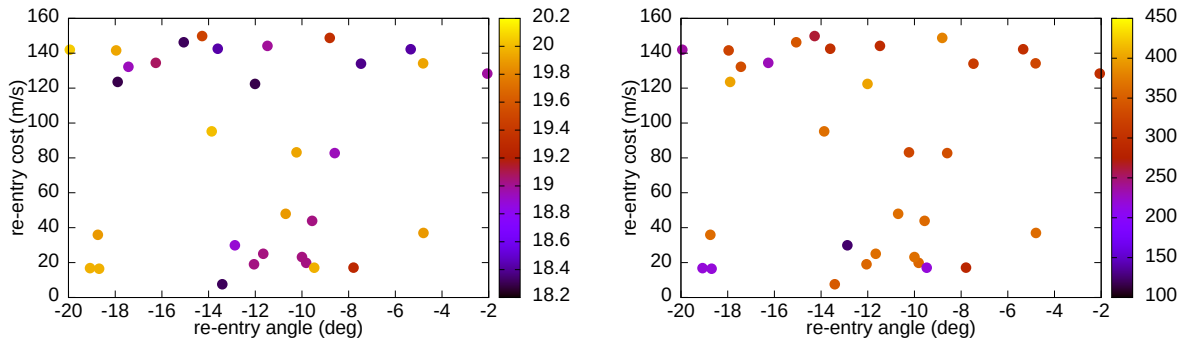

Figure 18. **Optimal solutions found for Gaia re-entry in terms of re-entry cost (m/s) and re-entry angle (deg), being the initial epoch on the LPO on January 23, 2014 at 00:00. The color bar on the left reports the initial epoch of the re-entry trajectory (left) and the total time of transfer in days (right).**

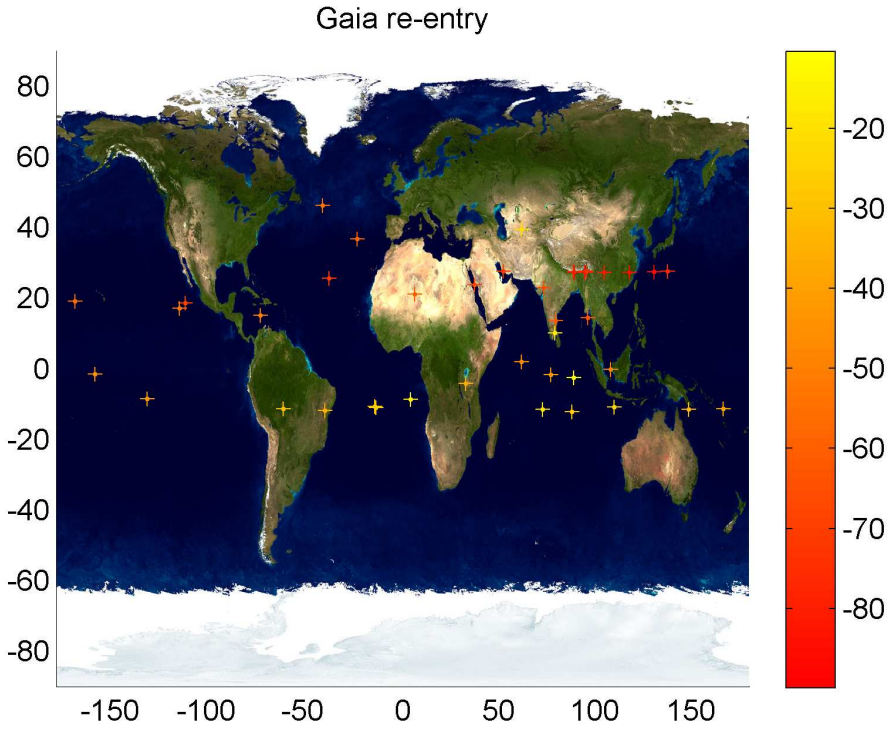

Figure 19. **Ground-track of the entry conditions (at 100 km) for the low-cost solutions ($\Delta v <$ 10 m/s) obtained for Gaia, taking as initial epoch on the LPO January 23, 2014 at 00:00. The color bar reports the corresponding angle of re-entry (deg).**

the maximum return from the payload. In May 2013[1] a disposal maneuver, actually the main of a

[1] `http://sci.esa.int/herschel/52797-herschel-status-report-05-2013/` last retrieval April 21, 2014.

series, of nominal magnitude of 113.732 m/s was performed to inject the s/c into a higher heliocentric orbit such that no-return to Earth is expected in 300 years at least. The alternative solutions proposed in this work would have required less propellant, but, according to the constraint imposed on the re-entry angle range, the disposal should have started earlier with thus a lower exploitation of the mission also from the science perspective. However, by relaxing the accepted interval of values for γ up to -40°, there exist re-entry trajectories for Herschel that can be considered feasible also in 2013 with respect to time of flight (not greater than 1 year) and Δv cost (less than 100 m/s).

Speaking more in general, following the outcome provided in this study, an Earth's re-entry can be considered as a disposal option for Herschel and SOHO-like missions. The nominal LPO associated with these cases allow almost no-cost transfers to Earth in a time of flight not demanding from an operational point of view. This possibility is ensured by the type of LPO chosen, i.e. halo or quasi-halo, rather than the out-of-plane amplitude. The Δv requirements are well below the expected available propellant at the end-of-life both for Herschel and SOHO. For SOHO many solutions presented have a cost less than 10 m/s. This means, in particular, that some propellant could be used for the last leg of the re-entry phase, that is, to design a semi-controlled re-entry which we propose to analyze in the future.

Concerning Gaia, the issue is more delicate, in the sense that they actually exist low-cost solutions, also within the very limited Δv budget at the end-of-life of the mission, but they have to be investigated in more detail. A systematic search of the optimal intersection position between trajectories belonging to different hyperbolic manifolds must be carried out. Preliminary simulations indicate that these connections join the unstable manifold associated with Gaia and the manifold of quasi-halo orbits with small out-of-plane amplitude.

In all the cases, the collision probability within LEO and GEO region can be considered as negligible, because of the low number of excursions within the protected regions (the LEO region in particular). Also, the re-entry option resembles the one leading to the Moon [2, 3] in terms of operations complexity and propellant need. Our feeling is, however, that the latter should be applied only if a significant extension of the scientific return is possible.

A future work will be focused on studying the last phase of the Earth re-entry, to describe the interaction with the ticker stages of the atmosphere. Moreover, the direction of the re-entry maneuver will be optimized to select the re-entry point on the Earth's surface and minimize the ground casualty risk.

Acknowledgments

This study was performed under the ESA Contract No. 4000107624/13/F/MOS under the supervision of Markus Landgraf as Technical Officer. The authors acknowledge the other members of the team: S. Soldini, F. Letizia, H. Lewis from the University of Southampton, A. Rossi, L. Faggioli, L. Dimare from SpaceDyS, W. van der Weg, M. Vetrisano, M. Vasile from the University of Strathclyde.

6. References

[1] Szebehely, V. Theory of orbits. Academic Press, New York, 1967.

[2] Colombo C. et al. "End-of-life disposal trajectories for Libration Point and Highly Elliptical Orbit Missions." Proceedings of the International Astronautical Congress, Beijing, Republic of China, IAC-13-A6.P.24. 2013.

[3] Colombo C. et al. "End-of-life disposal trajectories for Libration Point and Highly Elliptical Orbit Missions." Proceedings of the 2nd Conference on Dynamics and Control of Space Systems, Rome, Italy, IAA-AAS-DyCoSS2-14-03-01. 2014.

[4] Gómez, G. and Mondelo, J. M. "The dynamics around the collinear equilibrium points of the RTBP." Physica D, Vol. 157, pp. 283–321, 2001.

[5] Gómez, G., Llibre, J., Martínez, R., and Simó, C. Dynamics and Mission Design Near Libration Point Orbits – Volume 1: Fundamentals: The Case of Collinear Libration Points. World Scientific, Singapore, 2000.

[6] Gómez, G., Jorba, A., Masdemont, J., and Simó, C. Dynamics and Mission Design Near Libration Point Orbits – Volume 3: Advanced Methods for Collinear Points. World Scientific, Singapore, 2000.

[7] Koon, W., Lo, J., M.W. and. Marsden, and Ross, S. Dynamical Systems, the Three-Body Problem and Space Mission Design. Marsden Books, ISBN 978-0-615-24095-4, 2008.

[8] Alessi, E. M., Gómez, G., and Masdemont, J. J. "A motivating exploration on lunar craters and low-energy dynamics in the Earth–Moon system." Celestial Mechanics and Dynamical Astronomy, Vol. 107, No. 1-2, pp. 187–207, 2010.

[9] Standish, E. and Williams, J. G. "Orbital Ephemerides of the Sun, Moon, and Planets." `http://iau-comm4.jpl.nasa.gov/XSChap8.pdf`.

[10] Vallado, D. A. Fundamentals of Astrodynamics and Applications. Space Technology Library, Microcosm Press, Hawthorne, 2013.

[11] Montebruck, O. and Gill, E. Satellite Orbits. Model, Methods, and Applications. Springer, New York, 2001.

[12] IAU SOFA Board. "IAU SOFA Software Collection." Issue 2013-12-02, http://www.iausofa.org.

[13] Jorba, A. "Numerical computation of the normal behaviour of invariant curves of n-dimensional maps." Nonlinearity, Vol. 14, pp. 943–976, 2001.

[14] Colombo, C., Letizia, F., Alessi, E. M., and Landgraf, M. "End-of-life Earth re-entry for highly elliptical orbits: the INTEGRAL mission." The 24th AAS/AIAA Space Flight Mechanics Meeting, Santa Fe, New Mexico. 2014.